

氏 名	李 正 熙
授 与 学 位	博 士 (工 学)
学 位 授 与 年 月 日	平 成 8 年 3 月 26 日
学 位 授 与 の 根 拠 法 規	学 位 規 則 第 4 条 第 1 項
研 究 科 , 専 攻 の 名 称	東 北 大 学 大 学 院 工 学 研 究 科 (博 士 課 程) 機 械 工 学 専 攻
学 位 論 文 題 目	A Study of Loading Effect on A. C. Potential Drop for a Crack (き 裂 に 対 す る 交 流 電 位 差 に 及 ぼ す 荷 重 の 影 響 に 関 す る 研 究)
指 導 教 官	東 北 大 学 教 授 阿 部 博 之
論 文 審 査 委 員	東 北 大 学 教 授 阿 部 博 之 東 北 大 学 教 授 坂 真 澄 東 北 大 学 教 授 庄 子 哲 雄 東 北 大 学 教 授 林 一 夫

論 文 内 容 要 旨

Chapter 1 Introduction

A new method utilizing alternating current potential drop (ACPD) for experimental determination of the Mode I stress intensity factor, K_I , has been proposed by Saka et al. (1990). The major advantage of this technique is measuring the potential drop on the specimen surface, not near the crack tip. Since high frequency A-C current flows on the specimen surface and around the crack tip due to the skin effect, the potential drop which changes with the load gives significant information about K_I .

However the model of the change in potential drop due to load has not successfully been proposed. The model is needed to devise an effective way of the application of this technique and to clarify the mechanism of the change in potential drop. The purpose of this study is to model the change in potential drop due to load. Additionally the effects of the magnetic flux, the demagnetization and the crack length on the change in potential drop are examined.

Chapter 2 Model of the Change in Potential Drop Due to Load

The model of the change in potential drop due to load for ferromagnetic and paramagnetic materials is proposed for two limiting cases of the measuring system; one is without magnetic flux in the air and the other is with a large amount of the magnetic flux.

In the case without magnetic flux in the air, the measuring system may be considered as an electric circuit shown in Fig. 2-1, where L_1 is the internal self-inductance of the specimen, L_2 the self-inductance of the leads for measuring potential, L_3 the self-inductance of the leads for current supply, R the resistance of the specimen, Z the impedance of the lock-in amplifier, I the total current and I_1 the current flowing through Z . The measured potential drop E between A and B shown in Fig. 2-1 is

$$E = \sqrt{R^2 + (\omega L_1)^2} I_0 \quad (2-5)$$

where I_0 is the amplitude of I , ω angular frequency of the A-C current. From Eq. (2-5), the change in potential drop due to load may be caused by the changes in R and L_i .

In the case without magnetic flux in the air for paramagnetic materials, the changes in R and L_i are caused by the change in the current on the specimen surface.

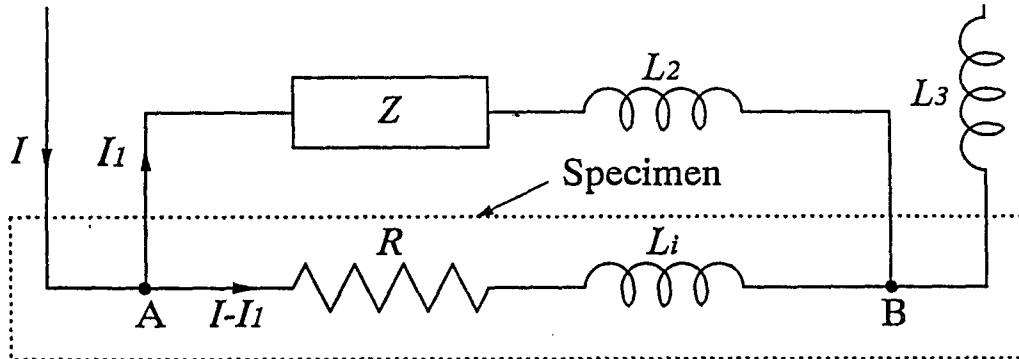


Fig. 2-1 Electric circuit model for the case without magnetic flux in the air

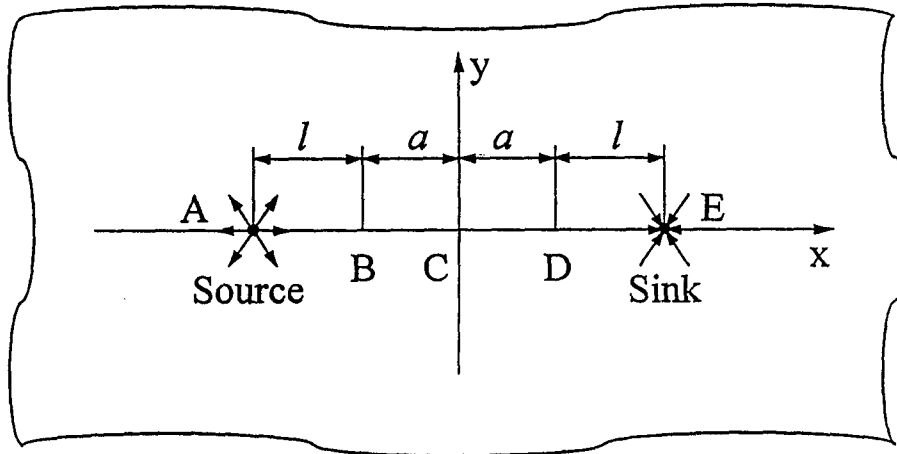


Fig. 2-2 (b) Unfolded two-dimensional crack and coordinates

Let us consider an unfolded infinite two-dimensional crack with length a and introduce a Cartesian coordinate system (x, y) as shown in Fig. 2-2 (b), where l is the distance between a current supply point and the crack mouth. Since ACPD is governed by the Laplace equation, the current input and output points can be considered as a source and a sink, respectively. Then the current density on the specimen surface is obtained as

$$J_x = \frac{I_0}{2\pi} \left\{ \frac{x+l+a}{(x+l+a)^2 + y^2} - \frac{x-l-a}{(x-l-a)^2 + y^2} \right\} \quad (2-6)$$

$$J_y = \frac{I_0}{2\pi} \left\{ \frac{y}{(x+l+a)^2 + y^2} - \frac{y}{(x-l-a)^2 + y^2} \right\}$$

where J_x and J_y are the components of the current density in the x and y directions, respectively. The current density at $y=0$ and near the sink, for example, is

$$J_x = -\frac{I_0}{2\pi} \frac{1}{x-l-a} \quad (2-7)$$

If a tensile load is applied to the cracked specimen, elongation due to elastic strain occurs particularly near the crack tip. The current density at a fixed distance x from the crack tip will change due to elastic strain as

$$J_x = \frac{I_0}{2\pi x_1 + b} \quad (2-10)$$

where x_1 is $l+a-x$ and b the elongation due to elastic strain, which is governed by K_I . It is found from Eq. (2-10) that the current density on the x axis decreases with increasing load. In the case without magnetic flux in the air, the magnetic flux through the surface made by the skin depth and the x axis decreases with increasing the load and hence L_i decreases. Therefore the change in potential drop decreases with increasing the tensile load for paramagnetic materials.

In the case without magnetic flux in the air for ferromagnetic materials, the changes in R and L_i are caused by the change in electromagnetic properties near the crack tip. It is well-known that the magnetization increases with increasing tensile load for steel specimen. With increasing the magnetization, R and L_i increase. Therefore the change in potential drop increases with increasing the load for ferromagnetic materials.

The measuring system with a large amount of magnetic flux can be considered as an electric circuit shown in Fig. 2-4, where L_1 is the self-inductance of the specimen, L_e the external self-inductance of the specimen, M_1 the mutual inductance between L_1 and L_3 , M_2 the mutual inductance between L_2 and L_3 and M_3 the mutual inductance between L_1 and L_2 . The measured potential drop E between C and D shown in Fig. 2-4 is

$$E = \sqrt{R^2 + \{\omega (L_i + L_e + M_1 + M_2 + M_3)\}^2} I_0 \quad (2-17)$$

From Eq. (2-17), the change in potential drop due to load may be caused by the changes in R , L_i , L_e , M_1 , M_2 and M_3 . Since R and L_i in the case with a large amount of magnetic flux are much less than L_e , M_1 , M_2 and M_3 , these terms can be neglected. If the leads for measuring potential drop and current supply are fixed on a plate so that their positions do not change even when a load is applied to the specimen, the mutual inductance M_2 will not change due to load. The change in potential drop is mainly caused by the changes in L_e , M_1 and M_3 which depend on the change in the current on the specimen surface.

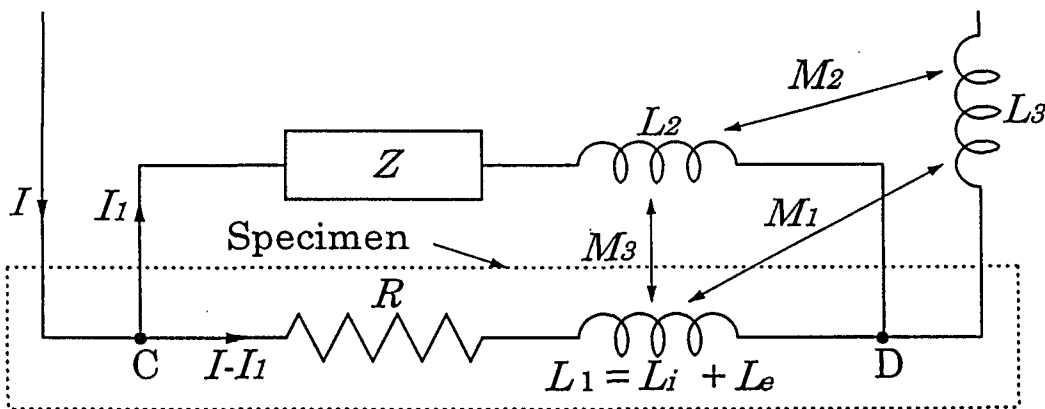


Fig. 2-4 Electric circuit model for the case with a large amount of magnetic Flux in the air

Let us consider a measuring system, the current density in the hatched region between the points of the current supply and coordinate system as shown in Fig. 2-5. It can be found from Eq. (2-6) that the absolute value of J , decreases with increasing the load. If the magnetic flux in the directions of 1 and 2 through Surfaces A_1 and A_2 shown in Fig. 2-5 increases, L_e , M_1 and M_3 increase. Since the magnetic flux through Surface A_2 in the direction 2 increases with decreasing the absolute value of J , the inductances L_e , M_1 and M_3 increase. Thus the change in potential drop increases with increasing the load in the case with a large amount of magnetic flux.

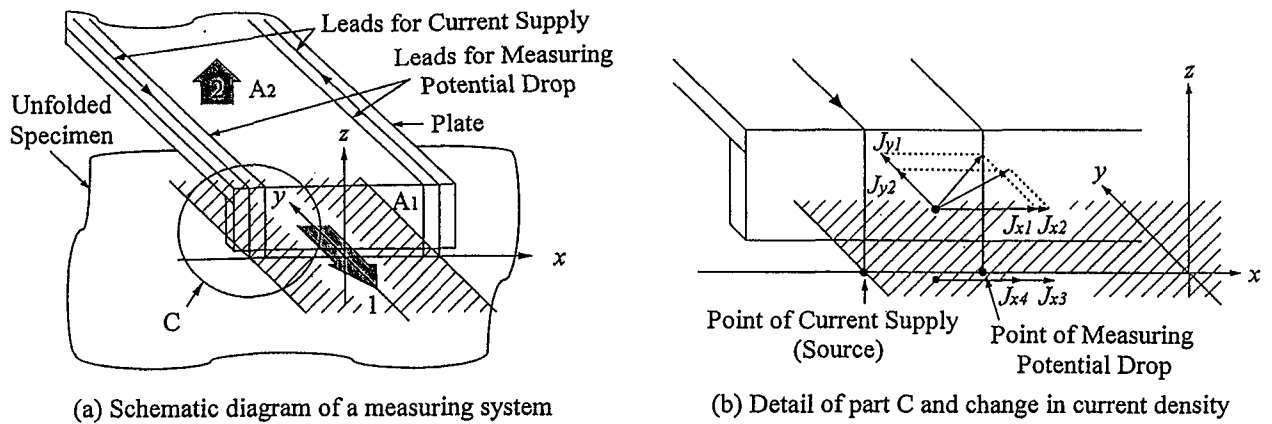


Fig. 2-5 A measuring system and change in current density due to load

Chapter 3 Method of Experiment

In order to verify the proposed model, the specimens and measuring systems were prepared to carry out the corresponding experiments. The specimens were made of steel (JIS G4013 SNCM439) as an example of ferromagnetic materials and aluminum alloy (JIS H4000 A2017) as an example of paramagnetic materials. The specimens were prepared with different total crack lengths, whose values were 6.1, 9.5 and 13.1 mm for steel and 6.1, 10.4 and 12.8 mm for aluminum alloy. For the measurement of potential drop, A-C current of 1 A with a frequency 10 kHz was used. Four kinds of the measuring systems designated SYSTEM 1 to SYSTEM 4 were made. In SYSTEM 1, the magnetic flux outside the specimen was removed by using the characteristic of the coaxial transmission line. In SYSTEM 4, the amount of the induced electromotive force was largely increased by extending the potential measuring lines to the vicinity of the current supply points and also winding the potential measuring lines as a coil.

Some specimens were demagnetized by decreasing slowly the amplitude of A-C current supplied to an electromagnet from 15 A-20 V to zero. Four kinds of the experiments designated Case A to Case D were carried out for each measuring system. In Case A and Case B, ACPD was measured by increasing and decreasing the load, respectively, applied to the specimens which were not demagnetized. In Case C and Case D, ACPD was measured by increasing and decreasing the load, respectively, applied to the demagnetized specimens. The specimens were demagnetized only at the state that the initial load had been applied to the specimen.

Chapter 4 Experimental Results

The relationship between the change in potential drop and that in K_1 was not linear in SYSTEMS 1 and 2 for steel. The change in potential drop obtained with SYSTEMS 1 and 2 for aluminum alloy decreased linearly with increasing K_1 . The amount of the change in potential drop due to the change in K_1 in SYSTEMS 1 and 2 was less than $1 \mu\text{V}$ for the range of K_1 examined. The relationship between the changes in potential drop and that in K_1 was linear in SYSTEMS 3 and 4 for respective materials. Also, the amount of the change in potential drop was largely increased. From these results, two facts can be found. First, the relationship between the change in potential drop and that in K_1 is linear without any treatment in the case of the measuring system with a large amount of magnetic flux. Second, if the amount of the magnetic flux in the measuring system is increased, a large amount of the change in potential drop can be measured.

The relationship between the change in potential drop and that in K_1 was linearized by demagnetization in the case of the measuring system without or with a little amount of magnetic flux in the air for steel. However demagnetization had almost no effect on the amount of the change in potential drop in the case of the measuring system with a large amount of magnetic flux in the air.

The changes in potential drop per unit change in K_I for all measuring systems were independent of the crack length for the respective materials.

Chapter 5 Model and Experiment

In order to verify the proposed model, the results obtained from the experiment were explained based on the model. The model can explain all the experimental results and hence it is valid.

Chapter 6 Application of the ACPD Technique to the Experimental Determination of K_I

For the application of the ACPD technique to the experimental determination of K_I in actual structures, it is needed to increase the amount of the change in potential drop due to load. To obtain a large amount of the change in potential drop, the measuring system should have a large amount of magnetic flux in the air. The additional necessary conditions required for the measuring system with a large amount of magnetic flux are making the area of the current supply points as small as possible, fixing the current supply points on the specimen surface and extending the measuring probe lines to the vicinity of the current supply points. A measuring system such as SYSTEM 4 is suitable for determining K_I experimentally because SYSTEM 4 has a large amount of magnetic flux and satisfies all these three additional necessary conditions.

Chapter 7 Conclusions

In order to devise an effective way of the application of ACPD technique to determining K_I experimentally and to clarify the mechanism of the change in potential drop due to load, the change in potential drop due to load was modeled for two limiting cases. To verify the proposed model, corresponding experiments were carried out.

The model can explain all the experimental results and hence it is valid. The change in potential drop is remarkably increased with increasing the magnetic flux of the measuring system. The change in potential drop was independent of the crack length. Demagnetization has almost no effect on the change in potential drop in the case with a large amount of the magnetic flux. An effective way of the application of ACPD technique to the experimental determination of K_I was found. That is increasing the magnetic flux of the measuring system such as SYSTEM 4. The cause of the change in potential drop was clarified. The cause of the change in potential drop due to load in the case with a large amount of magnetic flux was the change in the current on the specimen surface, which was caused by the elastic strain near the crack tip.

審 査 結 果 の 要 旨

破壊力学に基づく機器・構造物の健全性評価では、破壊力学パラメータの評価が不可欠である。代表的な破壊力学パラメータに応力拡大係数 K_I があり、 K_I を評価するための手法が従来から種々開発されてきた。とりわけ近年原理が発表されたばかりの、交流電位差法を用いて K_I を決定するという手法は、現場への適用可能性の点において優れており、その確立が待たれてきた。同手法の確立にあたっては、いかなる計測システムが有効であるかを解明することが肝要であった。

著者は、 K_I による電位差変化に関する理論モデルを考案し、これを踏まえ、有効な計測システムの提示に成功した。本論文はその内容をまとめたもので、全編7章からなる。

第1章は序論である。

第2章では、荷重による電位差変化の理論モデルを提案している。はじめに空気中に磁束がない計測システムを対象として、電位差変化をモデル化し、次に、空気中に大きな磁束を有する計測システムを対象とし、試験片表面上の電流の変化に起因して電位差が増加することを理論的に予測している。重要な成果である。

第3章では、第2章のモデルを検証するための実験方法について述べている。試験片の周囲から磁束を排除したシステムおよび空気中に大きな磁束を有するシステムの実現、ならびに消磁の影響を調べる目的で実施した実験の方法について説明を行っている。

第4章では、得られた実験結果を説明している。空気中に大きな磁束を有する計測システムでは、電位差変化が大きく、また消磁の有無によらず電位差変化が K_I の変化に比例し、かつ同関係はき裂長さに依存しないことを明らかにしている。有用な知見である。

第5章では、得られた実験結果を第2章のモデルにより説明し、モデルの妥当性を検証している。

第6章は実構造物に本手法を適用するにあたり、計測システムが具備すべき条件を述べている。これにより第3章で実現したような、空気中に大きな磁束を有するシステムが K_I の決定に有効であることを強調している。

第7章は結論である。

以上要するに本論文は、 K_I による交流電位差変化の機構を明らかにし、その成果に基づいて K_I を決定するための有効な計測システムを提案したもので、機械工学の発展に寄与するところが少なくない。

よって、本論文は博士（工学）の学位論文として合格と認める。